

# Performance Analysis of a Single Layer X-Band Frequency Selective Surface Based Spatial Filter Implementing Half Jerusalem Cross Slot

Harikrishna Paik<sup>1, 2, \*</sup> and Kambham Premchand<sup>1, 2</sup>

**Abstract**—This work proposes and experimentally evaluates a single layer bandpass frequency selective surface (FSS) that resonates at X-band (8–12 GHz). The metal plate of the unit cell has a half-Jerusalem cross slot of size  $0.15\lambda_0$ , where  $\lambda_0$  is the wavelength corresponding to 10 GHz centre frequency. The effects of unit cell parameters on filter response are analyzed through parametric analysis. The results reveal that the proposed bandpass FSS exhibits good polarization stability and angular stability at oblique angles up to  $45^\circ$ . Furthermore, negligible frequency deviations in both TE and TM polarizations have also been achieved using this structure. A prototype of the bandpass FSS was fabricated on an FR4 substrate to validate the proposed design which includes  $10 \times 10$  elements in a dimension of  $45 \text{ mm} \times 45 \text{ mm} \times 1.6 \text{ mm}$ . Measurements show that the bandpass FSS has a fractional bandwidth of 40% centered at 10 GHz from 8 GHz to 12 GHz. The unique feature of the proposed filter is its ability to operate in the whole X band (8–12 GHz) by tuning the filter elements.

## 1. INTRODUCTION

Frequency selective surfaces (FSSs) with filtering properties have been extensively studied at the microwave and millimeter frequencies in recent years. The FSSs typically consist of periodic arrangements of metallic patches or slots that can either transmit or reflect a desired incoming electromagnetic wave [1]. These FSSs have been often employed in the design of antenna, reflector, absorber, polarizer, and spatial filter [2–5]. In the recent times, FSSs as filters are extensively used in many microwave systems because of their low profile and ease of fabrication. Several approaches have been introduced to realize bandpass FSS with high selectivity and desired passband characteristics [6]. Furthermore, FSS based bandpass filters operating at C, X, Ka-Ku, and millimeterwaves with wide transmission band are often used in the applications, such as electromagnetic shielding, antenna sub-reflectors, and radome [7, 8]. Particularly, the filters in X band frequencies have gained popularity in military applications such as interceptor, missile guidance and control, and target tracking. Hence, the performance of a single layer wideband FSS bandpass filter operating in the X band frequencies has therefore been designed and analyzed in this paper.

During the past few decades, several FSS based bandpass spatial filters with different sizes, geometries, and filtering performance have been reported. Bandpass FSS using square loop slots [9], ground apertured annular ring resonators [10], multi layered cavities [11], aperture-coupled dual mode patch resonator [12], and cross aperture [13] are designed and analyzed. These filters have less angular stability and designed to operate at lower frequency bands [9–12]. Furthermore, the fractional bandwidths of the bandpass filters in [10, 11] are only 23% and 4.5%. The use of multilayer substrates, metallic vias, and lumped resistive elements adds complexity in these designs, making fabrication more difficult and lowering measurement accuracy. However, in the above designs, the operation of the FSS

---

*Received 16 September 2022, Accepted 1 December 2022, Scheduled 6 December 2022*

\* Corresponding author: Harikrishna Paik (pavan\_paik2003@yahoo.co.in).

<sup>1</sup> Department of Electronics and Communication Engineering, Veltech University, Chennai, India. <sup>2</sup> Department of Electronics and Communication Engineering, V R Siddhartha Engg. College, Vijayawada, India.

has been limited to lower frequency, narrow band operation, and multi-layered geometry. In this paper, a compact size and wide band slot resonator implemented using half Jerusalem cross is proposed to realize a bandpass FSS. The advantage of this structure is its simplicity, easy design, and compactness. The proposed filter comprises  $10 \times 10$  unit cells, which is modelled using Equivalent Circuit Model (ECM) approach, and dimensions of the unit cells are determined through optimization. The proposed work features greater angular stability and polarization stability than the designs in [9, 10, 12]. Furthermore, the proposed work shows less frequency deviation than the results in [13].

## 2. UNIT CELL GEOMETRY AND DESIGN

Figure 1(a) shows the 3-D view and top view of the proposed single layer bandpass FSS unit cell along with all the geometrical parameters.

As shown, the unit cell is composed of a single layer FSS with a half Jerusalem cross slot etched on the patch. This structure can resonate in the X-band by adjusting its geometrical dimensions and the distance between the unit cells. The average size of the unit cell is  $0.15\lambda_0$ , where  $\lambda_0$  represents the wavelength for center frequency of 10 GHz. The filter is designed on an FR4 substrate of thickness 1.6 mm with a dielectric constant of 4.4 and loss tangent of 0.02 using HFSS software. To verify circuit model performance, the Equivalent Circuit Model of the proposed bandpass FSS is established using ADS software and presented in Figure 1(b). As seen, the parallel inductor  $L_3$  and capacitor  $C_3$  represent the bandpass FSS unit cell. The circuit parameters  $L_1$ ,  $L_2$ ,  $C_1$ , and  $C_2$  represent the series resonant elements. The values of the filter elements are obtained by tuning and optimization as:  $L_1 = 0.884$  nH,  $C_1 = 4.51$  pF,  $L_2 = 0.933$  nH,  $C_2 = 2.795$  pF,  $L_3 = 1.668$  nH, and  $C_3 = 0.463$  pF. The simulation results determined by circuit simulation (in blue) and full-wave simulation (in red) are presented in Figure 2. It can be observed that the two results are in good agreement.

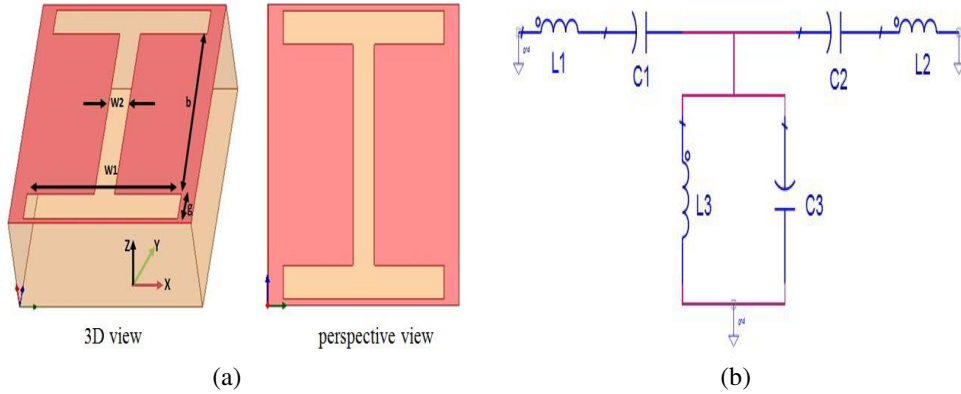


**Figure 1.** (a) Structure of unit cell, (b) equivalent circuit model.

## 3. EFFECT OF UNIT CELL GEOMETRY ON THE FILTER RESPONSE

To further analyze the filter responses, several unit cell geometrical parameters are varied, typically, dipole arm length ( $b$ ), thickness of lateral arm ( $g$ ), lateral arm width ( $W_1$ ), and thickness of the dipole arm ( $W_2$ ). It is depicted from Figure 3(a) that the filter resonates at the solution frequency of 10 GHz at  $b = 3.16$  mm and operates from 8.2 GHz to 11.6 GHz, as it deviates for other values of dipole length. From Figure 3(b), it is observed that as the value of  $g$  decreases from 0.5 mm to 0.35 mm, the resonance frequencies shift to higher value, and at  $g = 0.4$  mm, the unit cell has the impedance bandwidth of 3.8 GHz from 8 to 11.8 GHz.

The effects of variation in the parameters  $W_1$  and  $W_2$  on the filter response are shown in Figure 4. It is evident from Figure 4(a) that when  $W_1$  is varied from 4.1 mm to 3.2 mm, the resonant frequency shifts towards higher frequency due to the decrease in unit cell size. It is also clear that the proposed

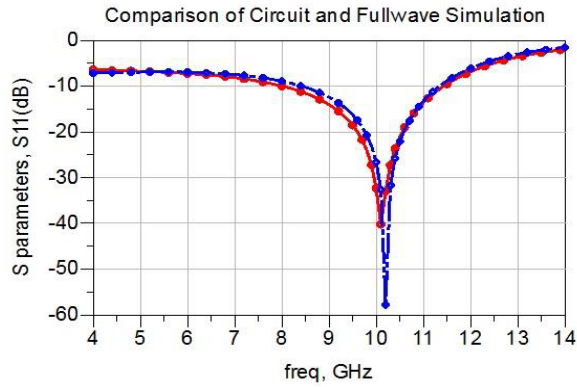


Figure 2. Performance comparison of circuit and full wave simulation.

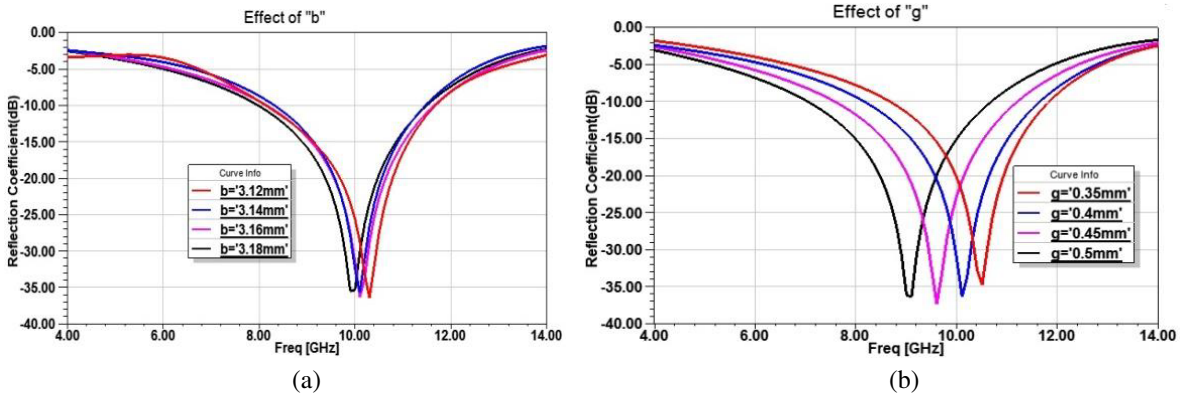


Figure 3. Unit cell reflection response for different values of (a) dipole arm length, (b) thickness of lateral arm.

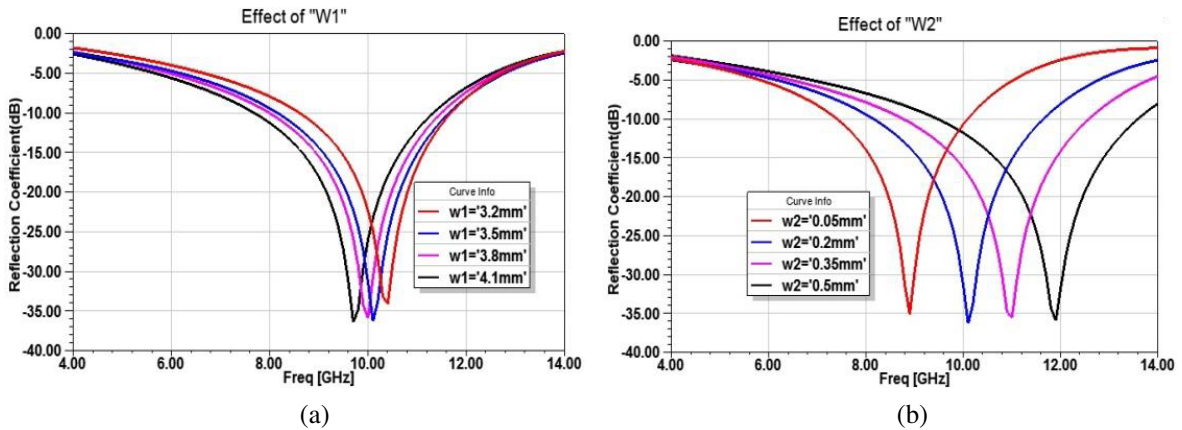


Figure 4. Unit cell reflection response for different values of (a) lateral arm width, (b) dipole arm thickness.

unit cell resonates at 10 GHz with reflection coefficient less than  $-10$  dB from 8 to 11.8 GHz. From Figure 4(b), it can be seen that the filter operates in the desired frequency band at  $W_2 = 0.2$  mm. Furthermore, the configuration has good control over the bandwidth because it does not change over the whole frequency of operation. From the above analysis, the dimensions of the unit cell are optimized as:  $d = 4.5$  mm,  $b = 3.16$  mm,  $g = 0.4$  mm,  $W_1 = 3.5$  mm,  $W_2 = 0.2$  mm and  $p = 5$  mm.

#### 4. EVALUATION OF FILTER PERFORMANCE

To have better insight, the performance of proposed filter in terms of polarization stability and angular stability is examined. The electric field is incident at the FSS structure with normal (horizontal polarization) and parallel (vertical polarization) directions, and response of the filter is observed. The electric field current distribution at a resonant frequency of 10 GHz is illustrated in Figure 5(a). As can be seen, for both the horizontal and vertical polarizations, the electric field is mainly concentrated at the lateral arms of the dipole. The magnitudes of the current are almost same for the two polarizations which show that the unit cell structure has good polarization stability because of equal effective path length across the dipole.

Further, the angular stability of the structure is evaluated at different incident angles between  $0^\circ$  and  $45^\circ$  for TE and TM polarizations as shown in Figure 5(b). It is observed that the filter resonates at 10 GHz with negligible frequency deviations for the angle of incident between  $0^\circ$  and  $45^\circ$  conforming the stable operation of the proposed design.

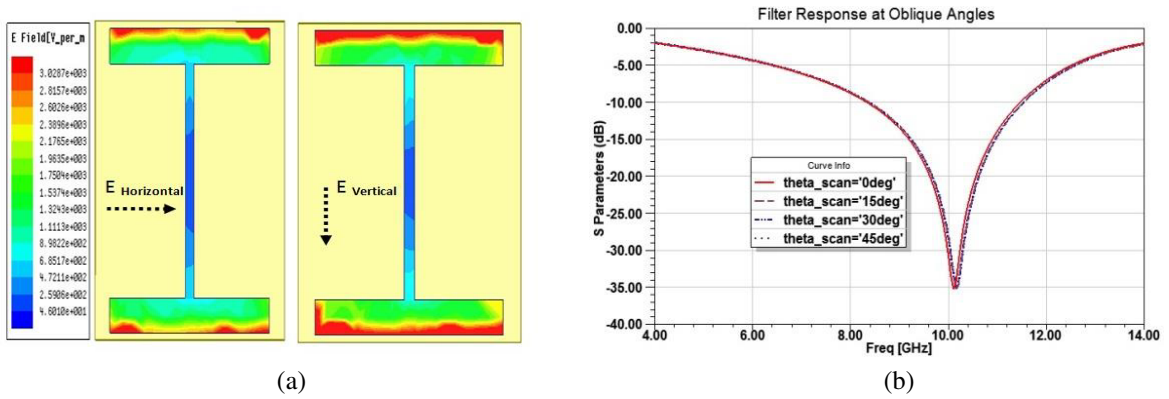


**Figure 5.** (a) Electric field distribution of operating frequency, (b) filter response at oblique angles.

### 5. EXPERIMENTAL RESULTS AND DISCUSSION

#### 5.1. Fabrication and Measurement Setup

A prototype of the proposed FSS bandpass filter is fabricated on an FR4 substrate which consists of  $10 \times 10$  elements to validate the simulation results. The overall dimension of the filter is  $45 \text{ mm} \times 45 \text{ mm}$ . Figure 6(a) shows a photograph of the fabricated structure and the measurement setup in the laboratory environment. As shown in the figure, two horn antennas along with Keysight N9918A vector network analyzer were set up to measure the filter performance which is similar to the one used in [14].

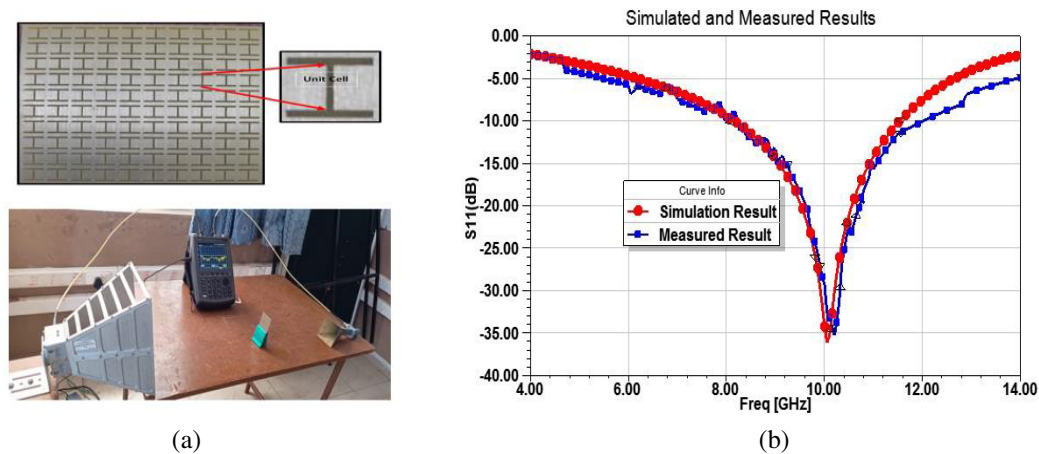
The simulated and measured frequency responses are compared as depicted in Figure 6(b). The measured results show that the prototype has a fractional bandwidth of 40% from 8 to 12 GHz at the center frequency of 10 GHz. It can be seen that they are in good agreement. However, the small differences between the measured and simulation results may be caused by the fault in fabrication and assembly errors.

#### 5.2. Performance Comparison

Table 1 compares the performance of the proposed design with the results reported in the literatures. It is noted that the proposed design has a better angular stability than the results in the literatures [9, 10, 12]. The unit cell size of this work is smaller than the elements in the reports [9, 10, 12] except in [13]. Furthermore, the  $-3 \text{ dB}$  bandwidth of the proposed design is 3.8 GHz which is considerably larger than the previous studies. From the above, it can be established that the proposed design features the advantages of compact size, high angular stability, and wide passband in the whole X band.

**Table 1.** Performance comparison.

Ref.	Frequency Band (GHz)	Unit cell type and size (mm)	No. of layers	Angular stability	-3 dB BW (GHz)
[9]	5.49–6.09	Square meander loop slot & 20	2	30°	0.60
[10]	7.2–7.9	Annular ring & 5	1	40°	0.7
[12]	12.6–14.8	Corner truncated square slot & 5.3	3	40°	2.2
[13]	28.75–30.15	Cross slot & 3.6	2	75°	1.4
This work	8–11.8 GHz	Half Jerusalem cross slot & 4.5	1	45°	3.8

**Figure 6.** Experimental Measurement. (a) Proto type and measurement set up, (b) measured and simulation results.

## 6. CONCLUSIONS

A compact size bandpass FSS with  $10 \times 10$  elements resonating in X-band frequencies with a fractional 3-dB passband bandwidth of 40% is reported. The proposed structure has a total dimension of  $1.67\lambda_0$  and a thickness of  $0.053\lambda_0$ , where  $\lambda_0$  denotes the wavelength of the centre frequency. With the aid of full-wave simulation, the performances of the proposed design were analyzed. It is established that the proposed bandpass FSS exhibits angular stability up to  $45^\circ$  and is polarization insensitive. This structure provided negligible frequency deviations for both TE and TM polarizations. The simple and symmetric response, wide pass band, good angular and polarization stability in both polarization modes of operations are the key features of the proposed filter.

## REFERENCES

1. Mei, P., G. F. Pedersen, and S. Zhang, "A broadband and FSS-based transmitarray antenna for 5G millimeter-wave applications," *IEEE Antenna and Wireless Propagation Letters*, Vol. 20, No. 1, 103–107, 2021.
2. Deng, Z. H., F. W. Wang, Y. H. Ren, K. Li, and B. J. Gao, "A novel wideband low-RCS reflector by Hexagon polarization rotation surfaces," *IEEE Access*, Vol. 7, 131527–131533, 2019.

3. Omar, A. A., H. Huang, and Z. Shen, "Absorptive frequency-selective reflection/transmission structures: A review and future perspectives," *IEEE Antenna and Propagation Magazine*, Vol. 62, No. 4, 62–74, 2020.
4. Lalbakhsh, A., M. U. Afzal, K. P. Esselle, and S. L. Smith, "All-metal wideband frequency-selective surface bandpass filter for TE and TM polarizations," *IEEE Transactions on Antennas Propagation*, Vol. 70, No. 4, 2790–2800, 2022.
5. Katoch, K., N. Jaglan, and S. D. Gupta, "A review on frequency selective surfaces and its applications," *2019 International Conference on Signal Processing and Communications (ICSC)*, 75–81, Noida, India, 2019.
6. Hussein, M., J. Zhou, Y. Huang, and B. A. Juboori, "A low-profile miniaturized second-order bandpass frequency selective surface," *IEEE Antennas and Wireless Propagation Letters*, Vol. 16, 2791–2794, 2017.
7. Tamoor, T., F. Ahmed, S. M. Q. A. Shah, T. Hassan, and N. Shoaib, "An FSS based stop band filter for EM shielding application," *2020 IEEE International Symposium on Electromagnetic Compatibility*, 978–980, Rome, Italy, 2020.
8. Mahima, P., B. Sangeetha, S. Narayan, and R. U. Nair, "EM design of hybrid-element FSS structure for radome application," *2016 Annual Indian Conference (INDICON 2016)*, 126–129, Bangalore, India, 2016.
9. Luo, G. Q., W. Yu, Y. Yu, X. H. Zhang, and Z. Liao, "Bandpass absorptive frequency-selective structure using double-sided parallel-strip lines," *IEEE Antennas and Wireless Propagation Letters*, Vol. 19, No. 9, 1596–1599, 2020.
10. Jin, C., Q. Lv, and R. Mittra, "Dual-polarized frequency selective surface with two transmission zeros based on cascaded ground apertured annular ring resonators," *IEEE Transactions on Antennas Propagation*, Vol. 66, No. 8, 4077–4085, 2018.
11. Chen, G. W., S. W. Wong, Y. Li, R. S. Chen, L. Zhang, A. K. Rashid, N. Xie, and L. Zhu, "High roll-off frequency selective surface with quasi-elliptic bandpass response," *IEEE Transactions on Antennas Propagation*, Vol. 69, No. 9, 5740–5749, 2021.
12. Xie, J. M., B. Li, Y. P. Lyu, and L. Zhu, "Single- and dual-band high-order bandpass frequency selective surfaces based on aperture-coupled dual-mode patch resonators," *IEEE Transactions on Antennas Propagation*, Vol. 69, No. 4, 2130–2141, 2021.
13. Chou, H. H. and G. J. Ke, "Narrow bandpass frequency selective surface with high level of angular stability at Ka-band," *IEEE Microwave Wireless Components Letters*, Vol. 31, No. 4, 361–364, 2021.
14. Yu, W., G. Q. Luo., Y. Yu, W. Cao, Y. Pan, and Z. Shen, "Dual-polarized band-absorptive frequency selective rasorber using meander-line and lumped resistors," *IEEE Transactions on Antennas and Propagation*, Vol. 67, No. 2, 1318–1322, 2019.